Photoacoustics 29 (2023) 100436

Contents lists available at ScienceDirect

Photoacoustics

journal homepage: www.elsevier.com/locate/pacs

Parts-per-billion-level detection of hydrogen sulfide based on doubly resonant photoacoustic spectroscopy with line-locking

Hui Zhang [a,b], Zhen Wang [c,d], Qiang Wang [a,b,*], Simone Borri [d], Iacopo Galli [d], Angelo Sampaolo [e], Pietro Patimisco [e], Vincenzo Luigi Spagnolo [e], Paolo De Natale [d], Wei Ren [c]

[a] State Key Laboratory of Applied Optics, Changchun Institute of Optics, Fine Mechanics and Physics, Chinese Academy of Sciences, Changchun 130033, China
[b] University of Chinese Academy of Sciences, Beijing 100049, China
[c] Department of Mechanical and Automation Engineering, The Chinese University of Hong Kong, New Territories, Hong Kong SAR, China
[d] CNR-INO – Istituto Nazionale di Ottica, and LENS – European Laboratory for Nonlinear Spectroscopy, 50019 Sesto Fiorentino, Italy
[e] PolySense Lab – Dipartimento Interateneo di Fisica, University and Politecnico of Bari, Via Amendola 173, Bari, Italy

ARTICLE INFO

Keywords:
Photoacoustic spectroscopy
Cavity-enhanced spectroscopy
Hydrogen sulfide
Trace gas detection
Molecular absorption line locking

ABSTRACT

We report on the development of a highly sensitive hydrogen sulfide (H_2S) gas sensor exploiting the doubly resonant photoacoustic spectroscopy technique and using a near-infrared laser emitting at 1578.128 nm. By targeting the R(4) transition of H_2S, we achieved a minimum detection limit of 10 part per billion in concentration and a normalized noise equivalent absorption coefficient of 8.9×10^{-12} W cm^{-1} Hz$^{-1/2}$. A laser-cavity-molecule locking strategy is proposed to enhance the sensor stability for fast measurement when dealing with external disturbances. A comparison among the state-of-the-art H_2S sensors using various spectroscopic techniques confirmed the record sensitivity achieved in this work.

1. Introduction

Hydrogen sulfide (H_2S) is a gas species of great importance for numerous application fields, such as environmental monitoring [1], petrochemical processes [2,3] and medical treatment [4], where its concentration or variation trend usually needs to be accurately measured. With characteristic odor of rotten eggs at ultralow concentration, H_2S is one of the most highly toxic, corrosive, and flammable gas, which can cause dizziness, nausea, eye injury, and even asphyxiation, shock or convulsions [3,5]. Apart from personal safety, H_2S can also corrode metallic equipment, resulting in economic losses [6,7]. Besides, H_2S not only is an indicator of food spoilage [8–10], but also has emerged as a endogenous signal molecule with crucial pathophysiological roles in cardiovascular function [11]. Very recently, ppb-level trace H_2S has also been used as a biomarker for the early diagnosis and therapy of lung diseases such like asthma [4]. Its quantitative and fast determination in the few parts-per-billion (ppb) concentration range is critically required in these multidisciplinary domains for fundamental or applied research but still remains challenging for reliable sensors.

With continuous contributions from the scientific community, different H_2S detection approaches emerge from simple colorimetric assays [12] to precise techniques, such as chromatography [13,14], metal-oxide semiconductor [15,16], nanoparticle [17], organic thin film [18], and laser spectroscopy [19]. Gas chromatography, as a commercial instrument, has been employed the most frequently, but it can hardly achieve atmospheric H_2S detection down to ppb level [14]. The electrochemical sensors show high sensitivity to H_2S with a ppb-level detection limit [15,16,18], but they are readily affected by temperature and humidity variations [14]. Tunable diode laser absorption spectroscopy (TDLAS), the most common laser spectroscopic mechanism for trace gas detection, highlights itself with unique advantages of high selectivity, high sensitivity, and fast response. With the assistance of a multipass cell (MPC) to extend the light-gas interaction length [21], TDLAS achieved trace H_2S measurement with a sensitivity of 80 ppb in mid-IR (8 μm) [19]. The absorption path length can be further increased to several kilometers by a high-finesse optical cavity [22–24]. Off-axis integrated cavity output spectroscopy (ICOS) [23] and cavity ring-down spectroscopy (CRDS), for instance, have contributed to breakthroughs in H_2S detection, particularly a detection limit of 20 ppb [25]. However, the technical limitations, such as limited dynamic range

* Corresponding author at: State Key Laboratory of Applied Optics, Changchun Institute of Optics, Fine Mechanics and Physics, Chinese Academy of Sciences, Changchun 130033, China.
E-mail address: wangqiang@ciomp.ac.cn (Q. Wang).

https://doi.org/10.1016/j.pacs.2022.100436
Received 23 October 2022; Received in revised form 22 November 2022; Accepted 8 December 2022
Available online 9 December 2022

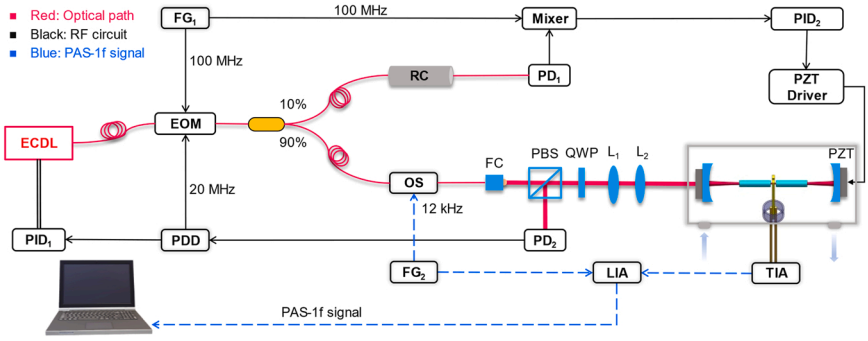

Fig. 1. Schematic configuration of doubly resonant PAS with the laser-cavity-molecule locking strategy. ECDL, external cavity diode laser; EOM, electro-optic modulator; $FG_{1,2}$, function generator; PDD, the Pound-Drever-Hall Detector; $PID_{1,2}$, proportion-integration-differentiation controller; PZT driver, piezo transducer driver; TIA, trans-impedance amplifier; LIA, lock-in amplifier; OS, optical switch; FC, fiber collimator; PBS, polarization beam splitter; QWP, quarter-wave plate; $L_{1,2}$, mode matching lens; $PD_{1,2}$, photodetector; RC, reference cell.

due to the intracavity absorption [26], etalon effects superposed on photodetectors [27], and bulky chamber with a large gas consumption, may restrict its wide applications out of laboratory.

Photoacoustic spectroscopy serves as an alternative option with wide dynamic range, excitation wavelength independence, and no need for photodetectors, which has been demonstrated for the detection of numerous inorganic and organic trace gases [20,28–41]. Particularly, exploiting a tiny quartz tuning fork (QTF) [42–45] as the acoustic transducer provides practical attraction with high sensitivity, good immunity to environmental acoustic noise, tiny size, low cost, and ultra-low gas consumption [46]. The acoustic signal scales linearly with laser power, rather than a long absorption path. Thus, by employing an erbium-doped fiber amplifier (EDFA) to boost the excitation laser power, a detection sensitivity of 17 ppb for H_2S was achieved at atmospheric pressure and room temperature [35]. The photoacoustic signal can also be efficiently enhanced by the employment of a multi-pass optical configuration [47] or the direct utilization of high intracavity power inside a laser resonator [48,49].

In recent years, optical resonators have proven to be a powerful tool, which can enhance the laser power by several orders of magnitude [50,51]. It is worth mentioning that a doubly resonant PAS-based gas sensor, by integrating an optical resonator and an acoustic resonator, achieved a record sensitivity of 10^{-13} cm^{-1} (NEA) and an unprecedent dynamic range of eight orders of magnitude simultaneously [52]. In that sensor, scanning of the whole spectra required slow frequency ramps or continuous relocking of the laser to the cavity in a stepwise manner. This affected the measurement time, stretching it up to several minutes. It is well known that in traditional PAS works, the measurement speed can be increased when the laser wavelength is locked to the selected molecular absorption lines [41,53]. In the cavity-enhanced PAS, this line locking method was lacking.

In this paper, we develop a highly sensitive H_2S sensor, which blends the doubly resonant PAS, an opto-acoustic resonance approach that can generate significantly enhanced photoacoustic waves, with a laser-cavity-molecule locking strategy, a spectroscopic method to stabilize the laser frequency. Rather than scanning the entire spectrum, the locking strategy enables the simultaneous locking of the laser frequency and the cavity mode to an absorption line, which yields a fast response and an enhancement of the system stability. Choosing a near-infrared absorption line (1578.128 nm) of H_2S as the investigation target, we demonstrate the continuous H_2S measurement with a noise equivalent concentration (NEC) of 10 ppb for integration time of 200 s, a normalized noise equivalent absorption (NNEA) coefficient of 8.9×10^{-12} W cm^{-1} $Hz^{-1/2}$, and a dynamic range of four orders of magnitude.

2. Experimental setup

Fig. 1 illustrates the sensor configuration for trace H_2S measurement. The double resonance structure is placed inside a vacuum chamber equipped with two wedged CaF_2 windows for optical access. An optical resonator, formed by a pair of cavity mirrors with a reflectivity exceeding 0.9985 and a radius of curvature of 50 mm, has been specifically arranged with a QTF detection system inside. The optical resonator has a length of 80 mm in this work, corresponding to a free spectral range (FSR) of 1.875 GHz. The intracavity laser beam (beam waist: 100 μm) propagates through an acoustic detection module with two on-beam acoustic resonators (inner diameter: 1.6 mm; length: 12.4 mm) and a custom QTF (prong space: 800 μm). This custom QTF, fabricated at *PolySense Lab*, has a resonant frequency of 12.452 kHz at 1 bar.

As shown in Fig. 1, the optical path is indicated by the red connecting lines. An external cavity diode laser (ECDL, CTL1550, TOPTICA Photonics) emitting at 1578.128 nm is used as the laser source to target the R(4) transition of H_2S. With a polarization-maintaining beam splitter, a small fraction of the laser (10 %) interrogates a reference cell filled with pure H_2S (see Appendix A) and impinges on PD_1. The rest of the laser (90 %), shaped by mode matching lenses, is coupled into the optical resonator for power buildup. The reflected laser beam, by the optical cavity, is picked out by a quarter-wave plate and a polarization beam splitter and then is detected by PD_2. The coupling efficiency of incident power has been achieved to be 93.8 % (see Appendix B) by using two mode matching lenses (focus length: $L_1 = 30$ mm and $L_2 = 50$ mm).

Black lines in Fig. 1 indicate the electrical connections used to perform the laser-cavity-molecule locking strategy. With the laser emission as the carrier frequency, two pairs of sidebands are simultaneously generated by an electro-optic phase modulator (EOM, iXblue Photonics). A Pound-Drever-Hall (PDH) error is demodulated by the PDD with a reference of 20 MHz [54]. Both the current feedback loop and piezo transducer (PZT) feedback loop of the ECDL are used to tightly lock the laser to the optical resonator via a proportional-integration-differentiation controller (PID_1) (FALC 110, TOPTICA Photonics). To perform the locking to the molecular absorption line, another pair of sidebands is generated by applying a 100 MHz modulation (FG_1) on the same EOM. By mixing the photodetector (PD_1) signal with a 100 MHz reference, the error signal is retrieved to PID-control a PZT actuator, which is attached to the rear cavity mirror. In this way, while the laser is locked to the cavity (PDH), the mismatch between laser and molecule line can be compensated by tuning the cavity length. As a result, both separate locking operations enable the simultaneous locking of the laser frequency and the cavity mode to the absorption line, the bandwidth of which are about 10 MHz and 5 kHz, respectively.

With the laser-cavity-molecule locking achieved, the laser intensity is modulated by a high-speed lithium niobate optical switch (NanoSpeed, Agiltron) at the resonance frequency (f_0) of the custom QTF. The signal from the QTF, converted to voltage by a trans-impedance amplifier, is finally demodulated at the frequency f_0 by a lock-in amplifier (MFLI 5 MHz, Zurich Instruments). The process for obtaining the photoacoustic signal is indicated by the blue dash lines in Fig. 1.

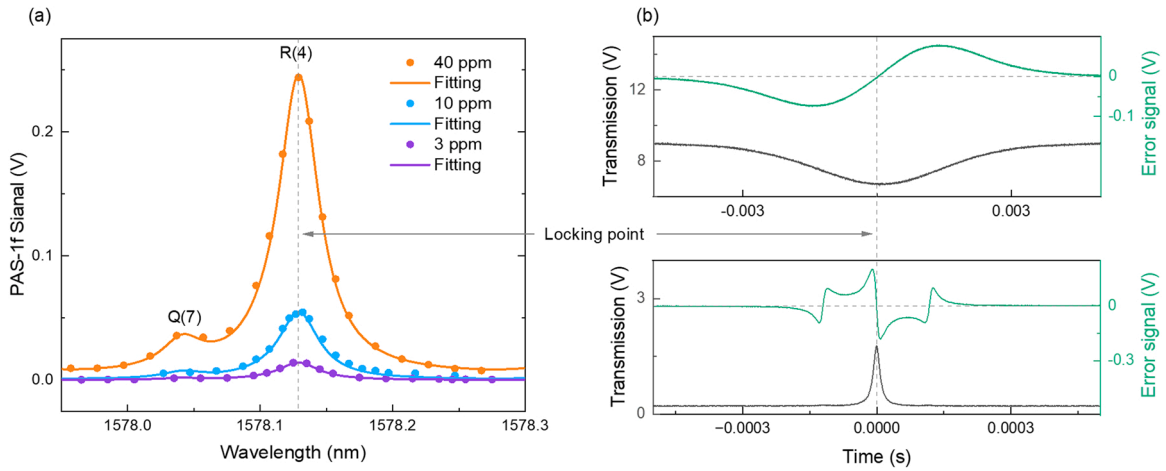

Fig. 2. The spectra of H_2S PAS-1f signals and error signals. (**a**) Representative PAS-1f signals of 40 ppm, 10 ppm, and 3 ppm H_2S:N_2 gas samples (1 bar). Solid line: the overall spectral fit of the experimental data with HITRAN database. (**b**) Typical transmissions (black curves) and error signals (green curves) for the laser-molecule locking (upper panel) and laser-cavity locking (bottom panel), respectively.

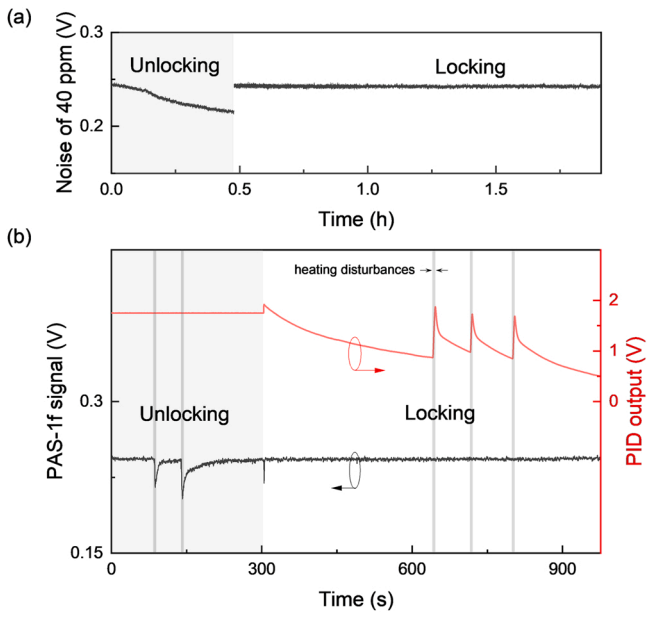

Fig. 3. Performance of molecular line-locking. (**a**) Under slowly varied room temperature, PAS-1f signal drifts without line-locking and remains long-term stable with line-locking. (**b**) Under external heating disturbances, PAS-1f signal drifts accordingly without line-locking while remains rather stable with real-time compensation for the cavity length. The PID output refers to the laser-molecule locking loop.

3. Results and discussion

3.1. Spectra of photoacoustic H_2S signals and error signals

Using the approach described in our recent work [52], the power buildup factor and acoustic enhancement factor are evaluated to be about 600 and 30, respectively. Before demonstrating the continuous photoacoustic measurement at the absorption transition, we measured the complete spectra of photoacoustic H_2S signals as well as error signals to determine the locking points. Fig. 2a presents the representative spectra of photoacoustic H_2S signals of three different concentrations at a pressure of 1 bar and room temperature (23 ± 1 ℃), measured in a stepwise manner in 5 min. The laser and the optical cavity were relocked for each measurement. The obtained data points can be fitted well with data obtained from the HITRAN database [55], and both the strong absorption line R(4) and the relatively small absorption line Q(7) of H_2S can be retrieved.

By scanning the laser wavelength, Fig. 2b shows the representative transmissions and error signals for the laser-molecule locking and laser-cavity locking, respectively. In the upper panel of Fig. 2b, the center zero-point corresponds to the peak of the PAS signal shown in Fig. 2a. In the bottom panel of Fig. 2b, the center zero-point of the PDH error signal corresponds to the peak of cavity transmission.

3.2. Molecular line-locking evaluation

To evaluate the performance of the laser-cavity-molecule locking strategy, a comparative test was performed, with and without molecular line-locking. With 40 ppm H_2S filled in the gas chamber, the laser wavelength was firstly tuned to the absorption line center without implementing the molecular line-locking. As shown in Fig. 3a, the PAS-1f signal decreases because the cavity length slowly drifts with the room temperature change. With the laser-cavity-molecule locking activated, the signal remains stable for more than 1.5 h. Besides, we purposely applied external heating on the gas chamber to introduce disturbance to the optical resonator length. With the polyimide heating film attached to the exterior surface of the gas chamber, a driver with a low power of 24 W was used for heating. Each external heating event lasted a short time (~ 3 s) and gas temperature inside the chamber had little change during the disturbance. However, the laser is very sensitive to the resonator length variation. Fig. 3b shows that the PAS-1f signal, with only laser-cavity locking, varies sharply due to the drift of laser wavelength with the heat disturbance. Conversely, when the laser-cavity-molecule locking is activated, the PAS-1f signal remains stable under the same external heating disturbance. The PID output shows the real-time compensation for the cavity length variation caused by the temperature change. From the activation of PID_2 at about 300 s, it starts to compensate for the drift caused by the previous external heating, and the three spikes show the compensations to three corresponding heating disturbances.

In this way, laser, optical cavity, and molecular absorption line are tightly locked with high immunity to laser wavelength drift and cavity length variation induced by environmental disturbances. The PAS-1f signal can thus be acquired continuously with no need for scanning the entire spectrum. Hence, the sensor response time is only limited by the integration time of QTF and the gas exchange rate.

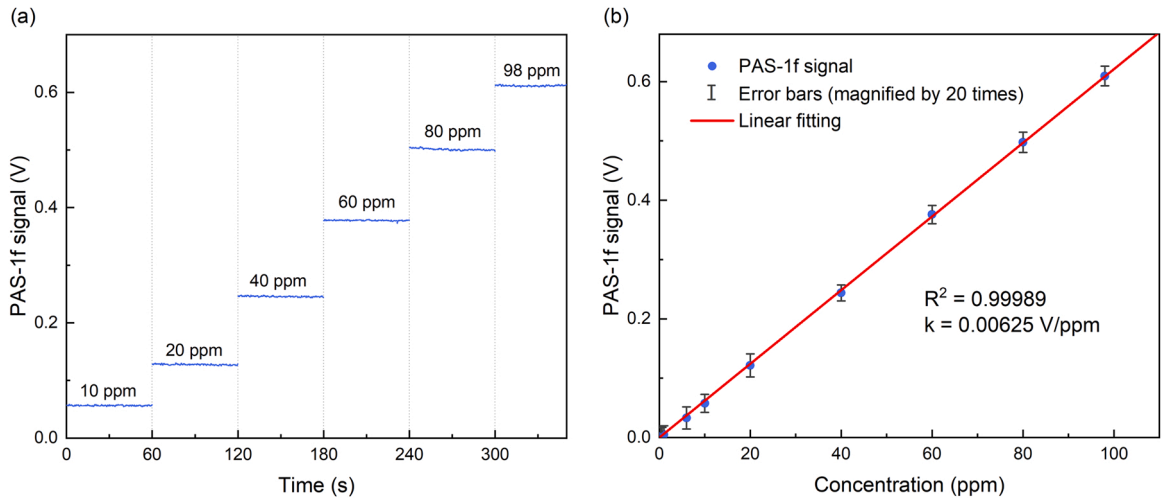

Fig. 4. (**a**) Stepwise measurement of the gas mixtures with increasing H_2S concentration. (**b**) PAS-1f signal versus H_2S concentration from 0.3 ppm to 98 ppm.

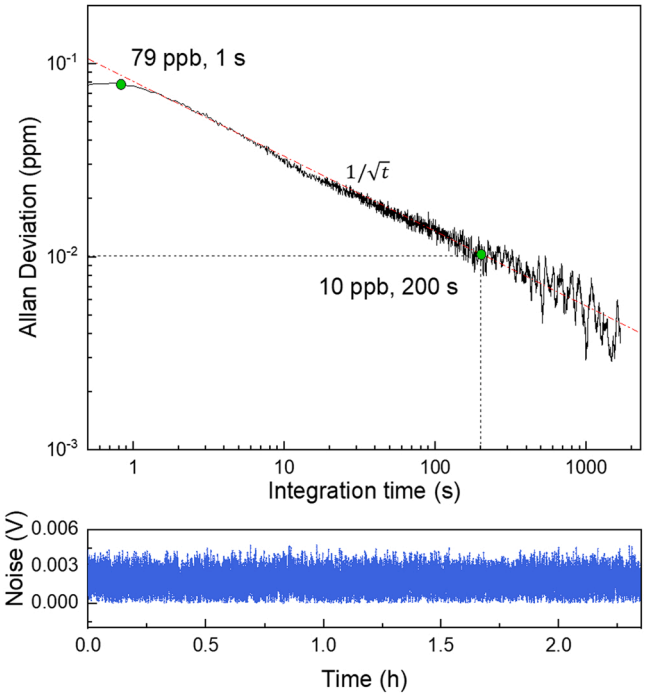

Fig. 5. Long-term stability analysis for pure N_2 gas sample. The upper panel shows the Allan-Werle deviation as a function of the acquisition time. The bottom panel depicts the raw data of noise measured for over 2 h. Note that the detection bandwidth is the same as the signal measurement (1 Hz).

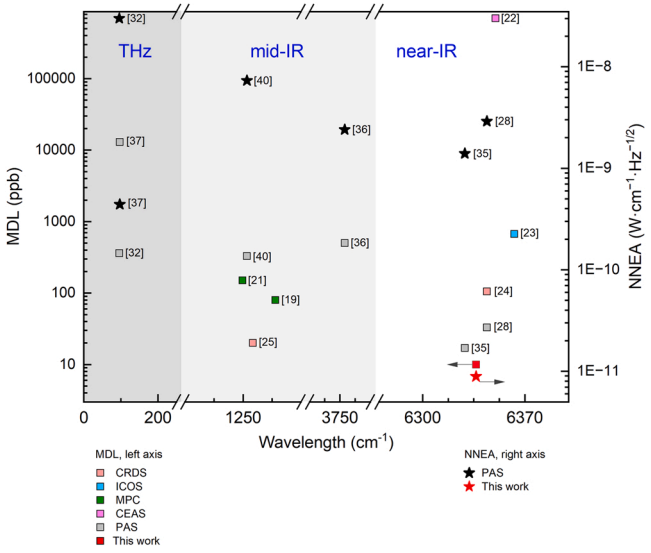

Fig. 6. Comparison among the state-of-the-art H_2S sensors, from near-IR to THz. All points labeled as squares refer to the MDL and those labeled as stars refer to the NNEA.

3.3. *Performance assessment of H_2S sensor*

After proving the high immunity to external disturbances and satisfactory system stability by the laser-cavity-molecule locking, we further evaluated its performance to detect trace H_2S gas. Considering the possible harm to the human body caused by high H_2S concentration, its concentration in the experimental measurement was set below 100 ppm. The mixtures were prepared by diluting a certified mixture of 98 ppm H_2S in pure nitrogen (purity 99.999 %) using a commercial gas mixer (Sonimix 7100, LNI Swissgas) at 1 bar. Fig. 4a shows the continuous measurement of the H_2S sample at different concentrations, with a duration time of 60 s for each concentration. As shown in Fig. 4b, the sensor responsivity is illustrated by plotting the PAS-1f signal as a function of the H_2S concentration between 0.3 ppm and 98 ppm. The vertical error bars are obtained by evaluating the uncertainty of the PAS-1f signal magnitude (1-σ standard deviation of the noise). Due to the extremely high signal-to-noise ratio (SNR), error bars are magnified by 20 times for the sake of clarity. The sensor shows a good linear response with a slope of 0.00625 V/ppm and an R-square value of 0.99989.

To investigate the minimum detection limit (MDL) and the long-term stability of the sensor, we performed an Allan-Werle deviation analysis of a measurement of pure N_2 for > 2 h with the laser-cavity-molecule locking activated. The results are shown in Fig. 5. The MDL is determined to be 79 ppb, also estimated as the NEC, at an integration time of 1 s, leading to a NNEA coefficient of 8.9×10^{-12} W cm^{-1} Hz$^{-1/2}$ with an incident optical power of 6.5 mW. The Allan-Werle deviation plot follows a $1/\sqrt{t}$ dependence, and the MDL can reach 10 ppb at an integration time of 200 s. The system is capable of averaging on a more than 1000 s time scale, which, as compared with previous cavity enhanced PAS works, also benefits from the high stability of the laser-cavity-molecule locking strategy [52]. The MDL of 10 ppb, together with the highest concentration of 98 ppm we employed, determines the linear dynamic range to be about 9.8×10^3, which could serve as a powerful analysis tool in many applications, such as medical diagnosis [4], food

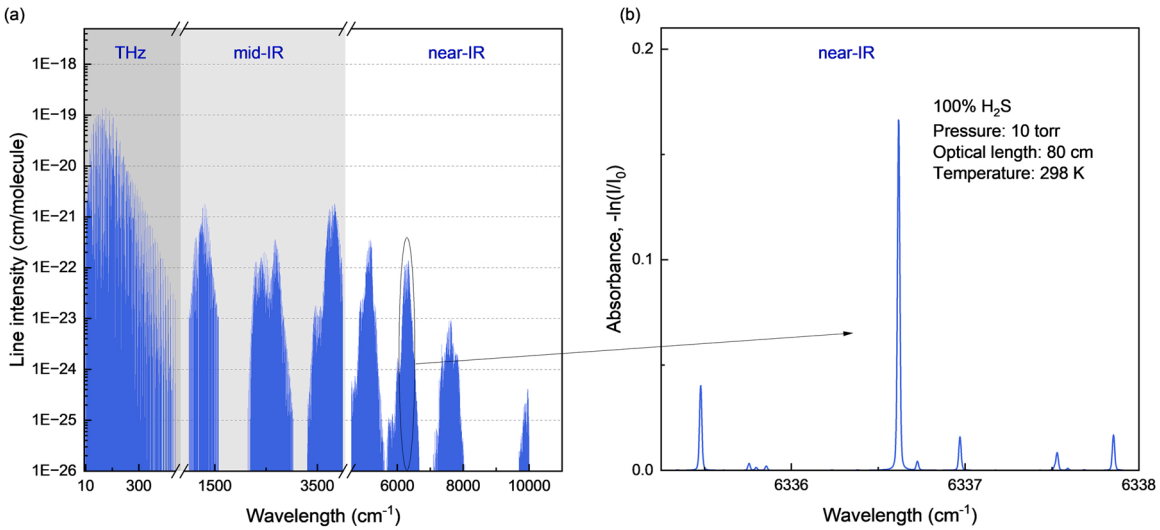

Fig. A1. **(a)** The line intensity of hydrogen sulfide in near-IR, mid-IR and THz spectral ranges. **(b)** The absorbance of reference cell in the vicinity of the chosen absorption line.

quality and safety monitoring [8,56], where H_2S measurements from few ppb to several tens of ppm level is needed.

In Fig. 6, we further compare the sensor performance in this work with the H_2S sensors based on other spectroscopic technologies, such as multipass-cell (MPC) assisted absorption spectroscopy [19,21], PAS (QEPAS included) [28,32,35–37,40], cavity-enhanced absorption (CEAS) [22], ICOS [23] and CRDS [24,25]. It is evident that this work shows the best performance in both MDL and NNEA among all reported H_2S sensors. Compared with the state-of-the-art PAS H_2S sensors, this sensor achieves an improvement of 1.5 times in MDL [35] and 50 times in NNEA [37]. Moreover, the sensor can potentially achieve a much better MDL with a commercially available optical power amplifier because of the linear relationship between the PAS sensitivity and the incident laser power [52].

4. Conclusion

In conclusion, we demonstrate highly sensitive H_2S gas sensing based on doubly resonant photoacoustic spectroscopy for fast H_2S detection. A strategy of laser-cavity-molecule locking is proposed to achieve continuous measurement. The sensor shows a linear responsivity and a good linear response for a concentration variation of four orders of magnitude. Furthermore, with an incident optical power of 6.5 mW, we have demonstrated a minimum detection limit of 79 ppb at 1 s integration time, corresponding to a NNEA coefficient of 8.9×10^{-12} W cm^{-1} Hz$^{-1/2}$ for H_2S measurement. By fully exploiting the stability of the proposed H_2S sensor, the integration time can be increased to 200 s, reaching a record MDL of 10 ppb. Moreover, the H_2S sensor can continuously operate at atmospheric pressure, which could enable fast and in-situ gas measurement. Further improvement of the detection sensitivity can be expected by employing a pair of cavity mirrors with a much higher reflectivity and by optimizing the on-beam acoustic resonators in their inner and outer diameters and tube length. Assessing the cross-relaxation of H_2S with other molecules, such as water vapor, to enhance the photoacoustic signal is also worth pursuing. Moreover, the availability of cavity mirrors for high cavity finesse and the development of locking techniques of a quantum cascade laser can contribute to the senor optimization in mid infrared to exploit the much stronger line strength.

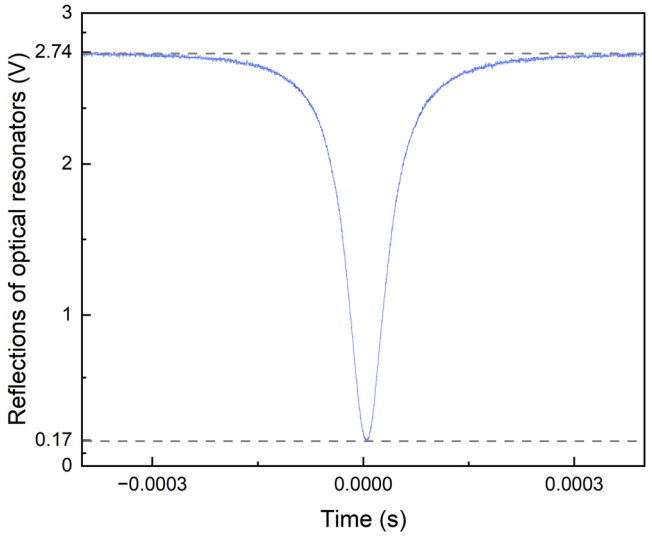

Fig. A2. Representative reflection signal from the optical resonator. The ground and valley voltage of the reflected signal from the optical resonator are 2.74 V and 0.17 V, respectively.

Declaration of Competing Interest

The authors declare that they have no known competing financial interests or personal relationships that could have appeared to influence the work reported in this paper.

Data Availability

Data will be made available on request.

Acknowledgements

This research was supported by the Second Comprehensive Scientific Investigation of the Qinghai-Tibet Plateau (2019QZKK020802), the National Natural Science Foundation of China (NSFC) (62005267), the Young Talent of Lifting Engineering for Science and Technology in Jilin, China (QT202106), and CIOMP International Cooperation Fund.

Appendix A. Hydrogen sulfide reference cell

As shown in Fig. A1a, the line intensity of H_2S strengthens gradually from the near-IR to the THz. Compared to THz and mid-infrared, near-IR

laser sources and optics are mature technologies, available on the market. Therefore, an appropriate absorption line of H_2S in the near infrared range, the R(4) transition at 1578.128 nm, is chosen as the investigation target. Hence, to perform laser frequency locking to the absorption line, the related parameters of the reference chamber need to be properly selected. On one hand, the lower the pressure is, the more accurate the reference wavelength can be, due to a narrower absorption line shape. On the other hand, the stronger the absorbance of the reference cell is, the higher the signal to noise ratio of the error signal for the laser-molecule locking will be. However, a low pressure may weaken the absorbance in the Beer-Lambert regime and Doppler broadening limits the absorption linewidth. As a tradeoff between line shape broadening and absorbance, a reference chamber (H_2S-15-0211914, Wavelength Reference; equivalent optical path: 80 cm; pressure: 10 torr) was customized with 100 % hydrogen sulfide filled. Fig. A1b shows its simulated absorbance spectrum in the range of 6335.2–6338 cm^{-1}.

Appendix B. Optical coupling efficiency

By scanning the wavelength of the ECDL, the reflected beam from the optical resonator can be detected by PD_2 shown in Fig. 1. The achieved optical coupling efficiency is determined to be 93.8 %, based on the recorded incident power for the fundamental resonator mode shown in Fig. A2. As the acoustic signal scales linearly with laser power, higher coupling efficiency will lead to a better sensitivity.

References

[1] F.I.M. Ali, F. Awwad, Y.E. Greish, S.T. Mahmoud, Hydrogen sulfide (H_2S) gas sensor: a review, IEEE Sens. J. 19 (2019) 2394–2407, https://doi.org/10.1109/JSEN.2018.2886131.

[2] A. Lagha, A. Ouederni, H. Ben Abdallah, Hydrogen sulfide removal from the waste gas of phosphoric acid plant, Environ. Prog. Sustain. Energy 39 (2020) 13304, https://doi.org/10.1002/ep.13304.

[3] W. Xie, H. Wang, M. Wang, Y. He, Genesis, controls and risk prediction of H_2S in coal mine gas, Sci. Rep. 11 (2021) 5712, https://doi.org/10.1038/s41598-021-85263-w.

[4] G.K. Kolluru, R.E. Shackelford, X. Shen, P. Dominic, C.G. Kevil, Sulfide regulation of cardiovascular function in health and disease, Nat. Rev. Cardiol. (2022) 1–17, https://doi.org/10.1038/s41569-022-00741-6.

[5] T.W. Lambert, V.M. Goodwin, D. Stefani, L. Strosher, Hydrogen sulfide (H_2S) and sour gas effects on the eye. A historical perspective, Sci. Total Environ. 367 (2006) 1–22, https://doi.org/10.1016/j.scitotenv.2006.01.034.

[6] D. Li, L. Zhang, J. Yang, M. Lu, J. Ding, M. Liu, Effect of H_2S concentration on the corrosion behavior of pipeline steel under the coexistence of H_2S and CO_2, Int. J. Miner. Metall. Mater. 21 (2014) 388–394, https://doi.org/10.1007/s12613-014-0920-y.

[7] A. Mirzaei, S.S. Kim, H.W. Kim, Resistance-based H_2S gas sensors using metal oxide nanostructures: a review of recent advances, J. Hazard. Mater. 357 (2018) 314–331, https://doi.org/10.1016/j.jhazmat.2018.06.015.

[8] A.M. Al Shboul, R. Izquierdo, Printed chemiresistive In_2O_3 nanoparticle-based sensors with ppb detection of H_2S gas for food packaging, ACS Appl. Nano Mater. 4 (2021) 9508–9517, https://doi.org/10.1021/acsanm.1c01970.

[9] S. Matindoust, M. Baghaei-Nejad, Z. Zou, L.-R. Zheng, Food quality and safety monitoring using gas sensor array in intelligent packaging, Sens. Rev. 36 (2016) 169–183, https://doi.org/10.1108/SR-07-2015-0115.

[10] K. Zhong, S. Zhou, X. Yan, X. Li, S. Hou, L. Cheng, X. Gao, Y. Li, L. Tang, A simple H_2S fluorescent probe with long wavelength emission: application in water, wine, living cells and detection of H_2S gas, Dyes Pigments 174 (2020), 108049, https://doi.org/10.1016/j.dyepig.2019.108049.

[11] B. Wang, C. Huang, L. Chen, D. Xu, G. Zheng, Y. Zhou, X. Wang, X. Zhang, The emerging roles of the gaseous signaling molecules NO, H_2S, and CO in the regulation of stem cells, ACS Biomater. Sci. Eng. 6 (2020) 798–812, https://doi.org/10.1021/acsbiomaterials.9b01681.

[12] A.P. Jarosz, T. Yep, B. Mutus, Microplate-based colorimetric detection of free hydrogen sulfide, Anal. Chem. 85 (2013) 3638–3643, https://doi.org/10.1021/ac303543r.

[13] I. Urriza-Arsuaga, M. Bedoya, G. Orellana, Unprecedented reversible real-time luminescent sensing of H_2S in the gas phase, Anal. Chem. 91 (2019) 2231–2238, https://doi.org/10.1021/acs.analchem.8b04811.

[14] S.K. Pandey, K.-H. Kim, K.-T. Tang, A review of sensor-based methods for monitoring hydrogen sulfide, TrAC Trends Anal. Chem. 32 (2012) 87–99, https://doi.org/10.1016/j.trac.2011.08.008.

[15] D. Li, Y. Tang, D. Ao, X. Xiang, S. Wang, X. Zu, Ultra-highly sensitive and selective H_2S gas sensor based on CuO with sub-ppb detection limit, Int. J. Hydrog. Energy 44 (2019) 3985–3992, https://doi.org/10.1016/j.ijhydene.2018.12.083.

[16] A.A. Shboul, A. Shih, M. Oukachmih, R. Izquierdo, Ppb sensing level hydrogen sulphide at room temperature using indium oxide gas sensors, in: Proceedings of the 2019 IEEE SENSORS, 2019, pp. 1–4.

[17] Y. Zhao, Y. Luo, Y. Zhu, Y. Sun, L. Cui, Q. Song, Sensitive colorimetric assay of H_2S depending on the high-efficient inhibition of catalytic performance of Ru nanoparticles, ACS Sustain. Chem. Eng. 5 (2017) 7912–7919, https://doi.org/10.1021/acssuschemeng.7b01448.

[18] Nagmani, D. Pravarthana, A. Tyagi, T.C. Jagadale, W. Prellier, D.K. Aswal, Highly sensitive and selective H_2S gas sensor based on TiO_2 thin films, Appl. Surf. Sci. 549 (2021), 149281, https://doi.org/10.1016/j.apsusc.2021.149281.

[19] M. Nikodem, K. Krzempek, D. Stachowiak, G. Wysocki, Quantum cascade laser-based analyzer for hydrogen sulfide detection at sub-parts-per-million levels, Opt. Eng. 57 (2017) 1, https://doi.org/10.1117/1.OE.57.1.011019.

[20] H. Moser, B. Lendl, Cantilever-enhanced photoacoustic detection of hydrogen sulfide (H_2S) using NIR telecom laser sources near 1.6 μm, Appl. Phys. B 122 (2016) 83, https://doi.org/10.1007/s00340-016-6355-6.

[21] H. Moser, W. Pölz, J.P. Waclawek, J. Ofner, B. Lendl, Implementation of a quantum cascade laser-based gas sensor prototype for sub-ppmv H_2S measurements in a petrochemical process gas stream, Anal. Bioanal. Chem. 409 (2017) 729–739, https://doi.org/10.1007/s00216-016-9923-z.

[22] S. Chandran, S. Mahon, A.A. Ruth, J. Braddell, M.D. Gutiérrez, Cavity-enhanced absorption detection of H_2S in the near-infrared using a gain-switched frequency comb laser, Appl. Phys. B 124 (2018) 63, https://doi.org/10.1007/s00340-018-6931-z.

[23] W. Chen, A.A. Kosterev, F.K. Tittel, X. Gao, W. Zhao, H_2S trace concentration measurements using off-axis integrated cavity output spectroscopy in the near-infrared, Appl. Phys. B 90 (2008) 311–315, https://doi.org/10.1007/s00340-007-2858-5.

[24] M. Siciliani de Cumis, S. Viciani, I. Galli, D. Mazzotti, F. Sorci, M. Severi, F. D'Amato, Note: an analyzer for field detection of H_2S by using cavity ring-down at 1.57 μm, Rev. Sci. Instrum. 86 (2015), 056108, https://doi.org/10.1063/1.4921582.

[25] M. Pal, S. Maithani, A. Maity, M. Pradhan, Simultaneous monitoring of ^{32}S, ^{33}S and ^{34}S isotopes of H_2S using cavity ring-down spectroscopy with a mid-infrared external-cavity quantum cascade Laser, J. Anal. At. Spectrom. 34 (2019) 860–866, https://doi.org/10.1039/C9JA00019D.

[26] D. Romanini, I. Ventrillard, G. Méjean, J. Morville, E. Kerstel, Introduction to cavity enhanced absorption spectroscopy, in: G. Gagliardi, H.-P. Loock (Eds.), Cavity-Enhanced Spectroscopy and Sensing. Springer Series in Optical Sciences, Springer, Berlin, Heidelberg, 2014, pp. 1–60 (ISBN 978-3-642-40003-2).

[27] A. Foltynowicz, F.M. Schmidt, W. Ma, O. Axner, Noise-immune cavity-enhanced optical heterodyne molecular spectroscopy: current status and future potential, Appl. Phys. B 92 (2008) 313–326, https://doi.org/10.1007/s00340-008-3126-z.

[28] K. Chen, B. Zhang, S. Liu, Q. Yu, Parts-per-billion-level detection of hydrogen sulfide based on near-infrared all-optical photoacoustic spectroscopy, Sens. Actuators B Chem. 283 (2019) 1–5, https://doi.org/10.1016/j.snb.2018.11.163.

[29] S. Palzer, Photoacoustic-based gas sensing: a review, Sensors 20 (2020) 2745, https://doi.org/10.3390/s20092745.

[30] Y. Ma, Recent advances in QEPAS and QEPTS based trace gas sensing: a review, Front. Phys. 8 (2020) 268, https://doi.org/10.3389/fphy.2020.00268.

[31] X. Yin, L. Dong, H. Wu, W. Ma, L. Zhang, W. Yin, L. Xiao, S. Jia, F.K. Tittel, Ppb-level H_2S detection for SF6 decomposition based on a fiber-amplified telecommunication diode laser and a background-gas-induced high-Q photoacoustic cell, Appl. Phys. Lett. 111 (2017), 031109, https://doi.org/10.1063/1.4987008.

[32] A. Sampaolo, C. Yu, T. Wei, A. Zifarelli, M. Giglio, P. Patimisco, H. Zhu, H. Zhu, L. He, H. Wu, et al., H_2S quartz-enhanced photoacoustic spectroscopy sensor employing a liquid-nitrogen-cooled THz quantum cascade laser operating in pulsed mode, Photoacoustics 21 (2021), 100219, https://doi.org/10.1016/j.pacs.2020.100219.

[33] H. Wu, A. Sampaolo, L. Dong, P. Patimisco, X. Liu, H. Zheng, X. Yin, W. Ma, L. Zhang, W. Yin, et al., Quartz enhanced photoacoustic H_2S Gas sensor based on a fiber-amplifier source and a custom tuning fork with large prong spacing, Appl. Phys. Lett. 107 (2015), 111104, https://doi.org/10.1063/1.4930995.

[34] H. Wu, L. Dong, H. Zheng, X. Liu, X. Yin, W. Ma, L. Zhang, W. Yin, S. Jia, F.K. Tittel, Enhanced near-infrared QEPAS sensor for sub-ppm level H_2S detection by means of a fiber amplified 1582 nm DFB laser, Sens. Actuators B Chem. 221 (2015) 666–672, https://doi.org/10.1016/j.snb.2015.06.049.

[35] H. Wu, L. Dong, X. Liu, H. Zheng, X. Yin, W. Ma, L. Zhang, W. Yin, S. Jia, Fiber-amplifier-enhanced QEPAS sensor for simultaneous trace gas detection of NH_3 and H_2S, Sensors 15 (2015) 26743–26755, https://doi.org/10.3390/s151026743.

[36] S. Viciani, M. Siciliani de Cumis, S. Borri, P. Patimisco, A. Sampaolo, G. Scamarcio, P. De Natale, F. D'Amato, V. Spagnolo, A quartz-enhanced photoacoustic sensor for H_2S trace-gas detection at 2.6 μm, Appl. Phys. B 119 (2015) 21–27, https://doi.org/10.1007/s00340-014-5991-y.

[37] V. Spagnolo, P. Patimisco, R. Pennetta, A. Sampaolo, G. Scamarcio, M.S. Vitiello, F. K. Tittel, THz quartz-enhanced photoacoustic sensor for H_2S trace gas detection, Opt. Express 23 (2015) 7574, https://doi.org/10.1364/OE.23.007574.

[38] A. Varga, Z. Bozóki, M. Szakáll, G. Szabó, Photoacoustic system for on-line process monitoring of hydrogen sulfide (H_2S) concentration in natural gas streams, Appl. Phys. B 85 (2006) 315–321, https://doi.org/10.1007/s00340-006-2388-6.

[39] A. Szabó, Á. Mohácsi, G. Gulyás, Z. Bozóki, G. Szabó, In situ and wide range quantification of hydrogen sulfide in industrial gases by means of photoacoustic spectroscopy, Meas. Sci. Technol. 24 (2013), 065501, https://doi.org/10.1088/0957-0233/24/6/065501.

[40] M. Siciliani de Cumis, S. Viciani, S. Borri, P. Patimisco, A. Sampaolo, G. Scamarcio, P. De Natale, F. D'Amato, V. Spagnolo, Widely-tunable mid-infrared fiber-coupled quartz-enhanced photoacoustic sensor for environmental monitoring, Opt. Express 22 (2014) 28222, https://doi.org/10.1364/OE.22.028222.
[41] A.A. Kosterev, L. Dong, D. Thomazy, F.K. Tittel, S. Overby, QEPAS for chemical analysis of multi-component gas mixtures, Appl. Phys. B 101 (2010) 649–659, https://doi.org/10.1007/s00340-010-4183-7.
[42] X. Liu, S. Qiao, G. Han, J. Liang, Y. Ma, Highly sensitive HF detection based on absorption enhanced light-induced thermoelastic spectroscopy with a quartz tuning fork of receive and shallow neural network fitting, Photoacoustics 28 (2022), 100422, https://doi.org/10.1016/j.pacs.2022.100422.
[43] S. Qiao, A. Sampaolo, P. Patimisco, V. Spagnolo, Y. Ma, Ultra-highly sensitive HCl-LITES sensor based on a low-frequency quartz tuning fork and a fiber-coupled multi-pass cell, Photoacoustics 27 (2022), 100381, https://doi.org/10.1016/j.pacs.2022.100381.
[44] F. Sgobba, A. Sampaolo, P. Patimisco, M. Giglio, G. Menduni, A.C. Ranieri, C. Hoelzl, H. Rossmadl, C. Brehm, V. Mackowiak, et al., Compact and portable quartz-enhanced photoacoustic spectroscopy sensor for carbon monoxide environmental monitoring in urban areas, Photoacoustics 25 (2022), 100318, https://doi.org/10.1016/j.pacs.2021.100318.
[45] A. Zifarelli, R. De Palo, P. Patimisco, M. Giglio, A. Sampaolo, S. Blaser, J. Butet, O. Landry, A. Müller, V. Spagnolo, Multi-gas quartz-enhanced photoacoustic sensor for environmental monitoring exploiting a vernier effect-based quantum cascade laser, Photoacoustics 28 (2022), 100401, https://doi.org/10.1016/j.pacs.2022.100401.
[46] L. Dong, A.A. Kosterev, D. Thomazy, F.K. Tittel, QEPAS spectrophones: design, optimization, and performance, Appl. Phys. B 100 (2010) 627–635, https://doi.org/10.1007/s00340-010-4072-0.
[47] S. Qiao, Y. Ma, P. Patimisco, A. Sampaolo, Y. He, Z. Lang, F.K. Tittel, V. Spagnolo, Multi-pass quartz-enhanced photoacoustic spectroscopy-based trace gas sensing, Opt. Lett. 46 (2021) 977–980, https://doi.org/10.1364/OL.418520.
[48] V.S. Starovoitov, J.F. Kischkat, M.P. Semtsiv, W.T. Masselink, Intracavity photoacoustic sensing of water vapor with a continuously tunable external-cavity quantum-cascade laser operating near 5.5 μm, Opt. Lett. 41 (2016) 4955–4958, https://doi.org/10.1364/OL.41.004955.
[49] Q. Wang, Z. Wang, W. Ren, P. Patimisco, A. Sampaolo, V. Spagnolo, Fiber-ring laser intracavity QEPAS gas sensor using a 7.2 kHz quartz tuning fork, Sens. Actuators B Chem. 268 (2018) 512–518, https://doi.org/10.1016/j.snb.2018.04.139.
[50] P. Patimisco, S. Borri, I. Galli, D. Mazzotti, G. Giusfredi, N. Akikusa, M. Yamanishi, G. Scamarcio, P. De Natale, V. Spagnolo, High-finesse optical cavity coupled with a quartz-enhanced photoacoustic spectroscopic sensor, Analyst 140 (2015) 736–743, https://doi.org/10.1039/c4an01158a.
[51] Z. Wang, Q. Wang, W. Zhang, H. Wei, Y. Li, W. Ren, Ultrasensitive photoacoustic detection in a high-finesse cavity with Pound–Drever–Hall locking, Opt. Lett. 44 (2019) 1924–1927.
[52] Z. Wang, Q. Wang, H. Zhang, S. Borri, I. Galli, A. Sampaolo, P. Patimisco, V. L. Spagnolo, P. De Natale, W. Ren, Doubly resonant sub-ppt photoacoustic gas detection with eight decades dynamic range, Photoacoustics 27 (2022), 100387, https://doi.org/10.1016/j.pacs.2022.100387.
[53] H. Zhang, W. Jin, M. Hu, M. Hu, J. Liang, Q. Wang, Investigation and optimization of a line-locked quartz enhanced spectrophone for rapid carbon dioxide measurement, Sensors 21 (2021) 5225, https://doi.org/10.3390/s21155225.
[54] M. Nickerson, A Review of Pound-Drever-Hall Laser Frequency Locking, JILA Univ. Colo. NIST, 2019.
[55] I.E. Gordon, L.S. Rothman, C. Hill, R.V. Kochanov, Y. Tan, P.F. Bernath, M. Birk, V. Boudon, A. Campargue, K.V. Chance, et al., The HITRAN2016 molecular spectroscopic database, J. Quant. Spectrosc. Radiat. Transf. 203 (2017) 3–69, https://doi.org/10.1016/j.jqsrt.2017.06.038.
[56] E. Tournie, L. Cerutti, Mid-Infrared Optoelectronics: Materials, Devices, and Applications, Woodhead Publishing, 2019 (ISBN 978-0-08-102738-7).

Hui Zhang received his BEng degree from Ocean University of China in 2019. He is currently a PhD candidate at Changchun Institute of Optics, Fine Mechanics and Physics, Chinese Academy of Sciences. His recent research focuses on photoacoustic gas sensing.

Zhen Wang is currently a research assistant professor at the Chinese University of Hong Kong. He received his Ph.D. degree from the Chinese University of Hong Kong. After that, he worked as a postdoc at the National Institute of Optics (CNR-INO) in Italy and a visiting scholar at Changchun Institute of Optics, Fine Mechanics and Physics, Chinese Academy of Science. His research interests are trace gas sensing and laser spectroscopy.

Qiang Wang is currently a professor at Changchun Institute of Optics, Fine Mechanics and Physics, Chinese Academy of Sciences. He received his B.S. degree in Electronic Science and Technology in 2011 and Ph.D. degree in Optical Engineering in 2016 from Shandong University. After his graduate study, he worked as a postdoctoral fellow at the Chinese University of Hong Kong and Max Planck Institute of Quantum Optics successively. His recent research interests are laser spectroscopy, optical sensing, and engineering application of trace gas analysis in the atmosphere, deep sea, and public health.

Simone Borri has completed his Ph.D. in 2007 from University of Firenze, Italy. He is researcher at CNR-National Institute of Optics since 2010. He worked as researcher for LENS, the European Laboratory for Nonlinear Spectroscopy, and IFN, the italian Institute for Photonics and Nanotechnologies. His area of expertize includes the development of narrow-linewidth metrological-grade coherent sources and techniques for high-sensitivity and high-precision molecular spectroscopy in the mid infrared.

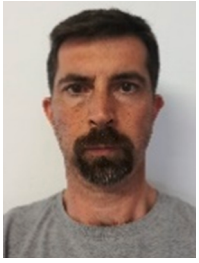

Iacopo Galli is currently a researcher of National Institute of Optics of the Italian National Research Council (CNR-INO). He received his Ph.D. degree in physics from University of Florence in 2009. Since 2009 he works in CNR-INO, first as post-doctoral researcher and today as researcher. In 2016 he have co-founded a spin-off of the National Research Council named ppqSense, the core business of the company is the radiocarbon detection with SCAR technique. His current research interests include nonlinear optics, high-sensitivity and high-precision infrared laser spectroscopy, gas sensing, frequency metrology, and quantum-cascade lasers characterization and stabilization.

Angelo Sampaolo obtained his Master degree in Physics in 2013 and the Ph.D. Degree in Physics in 2017 from University of Bari. He was an associate researcher in the Laser Science Group at Rice University from 2014 to 2016 and associate researcher at Shanxi University since 2018. Since May 2017, he was a Post-Doctoral Research associate at University of Bari and starting from December 2019, he is Assistant Professor at Polytechnic of Bari. His research activity has included the study of the thermal properties of heterostructured devices via Raman spectroscopy. Most recently, his research interest has focused on the development of innovative techniques in trace gas sensing, based on Quartz-Enhanced Photoacoustic Spectroscopy and covering the full spectral range from near-IR to THz. His achieved results have been acknowledged by a cover paper in Applied Physics Letter of the July 2013 issue.

Pietro Patimisco obtained the Master degree in Physics (cum laude) in 2009 and the Ph.D. Degree in Physics in 2013 from the University of Bari. Since 2018, he is Assistant professor at the Technical University of Bari. He was a visiting scientist in the Laser Science Group at Rice University in 2013 and 2014. Dr. Patimisco's scientific activity addressed both micro-probe optical characterization of semiconductor optoelectronic devices and optoacoustic gas sensors. Recently, his research activities included the study and applications of trace-gas sensors, such as quartz enhanced photoacoustic spectroscopy and cavity enhanced absorption spectroscopy in the mid infrared and terahertz spectral region, leading to several publications, including a cover paper in Applied Physics Letter of the July 2013 issue.

Vincenzo Luigi Spagnolo obtained the Ph.D. in physics in 1994 from University of Bari. From 1997 to 1999, he was researcher of the National Institute of the Physics of Matter. Since 2004, he works at the Technical University of Bari, formerly as assistant and associate professor and now as full Professor of Physics. Starting from 2019, he become Vice-Rector of the technical university of Bari - Deputy to Technology Transfer. He is the director of the joint-research lab PolySense between Technical University of Bari and THORLABS GmbH, fellow member of SPIE and senior member of OSA. His research interests include optoacoustic gas sensing and spectroscopic techniques for realtime monitoring. His research activity is documented by more than 220 publications and 3 filed patents. He has given more than 50 invited presentations at international conferences and workshops.

Paolo De Natale is research director at the National Institute of Optics-INO (Italian CNR) and member of the Directive Council of LENS, Firenze, Italy. In the years 2007–2021 was director of the National Institute of Optics of the Italian National Research Council (INO-CNR, former INOA). He is the Italian representative in the Quantum Community Network (QCN) Board of the EU Flagship on Quantum Technologies and in the Optronics CapTech of the European Defense Agency-EDA. Scientific interests include photonics, atomic and molecular physics, nonlinear optics and quantum technologies. He is author of more than 360 publications, owns 9 patents and is a co-founder of two former CNR spin-off companies, ppqSense srl and QTI srl. He is Fellow of IEEE (since 2011) and OSA (since 2015).

Wei Ren received the B.S. degree in Mechanical Engineering and M.S. degree in Optical Engineering from Tsinghua University in 2006 and 2008, respectively. He received the Ph.D. degree in Mechanical Engineering from Stanford University in 2013. He was awarded the Robert A. Welch Foundation post-doctoral fellowship to work in the Department of Electrical and Computer Engineering at Rice University in 2013–14. Dr. Ren is now an associate professor in the Department of Mechanical and Automation Engineering at the Chinese University of Hong Kong. His research to date has resulted in more than 70 peer-reviewed journal publications in laser spectroscopy, optical sensing, and chemical kinetics. He is currently the co-editor of Springer journal Applied Physics B. Prof. Ren is the senior member of OSA, and member of SPIE and the Combustion Institute.